Pakistan Veterinary Journal

ISSN: 0253-8318 (PRINT), 2074-7764 (ONLINE)
DOI: 10.29261/pakvetj/2026.116

RESEARCH ARTICLE

The Efficacy and Mechanism of *Prunus mume* Ethanol Extract in Preventing and Treating *Salmonella spp* Infection in Mice

Yang Yuai[1,#,*], Hu Miao[1,#,*], Li Jiayi[1,#], Chen Xiao[1], Wei Kang[1], Rana A. Alghamdi[2,3], Maha Abdullah Momenah[4], Yasser S. Mostafa[5] and Sun Yongke[1,*]

[1]College of Veterinary Medicine, Yunnan Agricultural University, Kunming 650201, Yunnan Province, China; [2]Department of Chemistry, Science and Arts College, King Abdulaziz University, Rabigh, Saudi Arabia; [3]Regenerative Medicine Unit, King Fahd Medical Research Centre, King Abdulaziz University, Jeddah, Saudi Arabia; [4]Department of Biology, College of Science, Princess Nourah bint Abdulrahman University, P.O. Box 84428, Riyadh 11671, Saudi Arabia; [5]Department of Biology, College of Science, King Khalid University, Abha P.O. Box 9004, Saudi Arabia. [#]These authors contributed equally to this article
*Corresponding author: yangyuai2008@126.com; sunyongke@126.com

ARTICLE HISTORY (26-278)

Received: March 27, 2026
Revised: May 11, 2026
Accepted: May 18, 2026
Published online: May 20, 2026

Key words:
Antioxidant
Diarrhea
Gut microbiota
Inflammation
Prunus mume polysaccharide
Salmonella spp

ABSTRACT

This study evaluated the protective effect of *Prunus mume* polysaccharide (PMP) against Salmonella spp.-induced enteritis in mice. Twenty-four ICR mice were randomly assigned to a control group (CD), model group (MD), and PMP treatment group (TD), with 8 mice in each group. Mice in the TD group received PMP (100mg/kg) by oral gavage for 14 consecutive days, while those in the CD and MD groups received an equal volume of normal saline. On day 14, mice in the MD and TD groups were challenged with *Salmonella spp*. (1×10^7 CFU/kg), and samples were collected 24h later. Compared with the MD group, PMP treatment alleviated body weight loss, reduced splenomegaly and intestinal bacterial burden, and attenuated jejunal and ileal mucosal injury. PMP significantly increased serum superoxide dismutase, glutathione peroxidase and total antioxidant capacity and decreased interleukin-6 ($P<0.05$). Gut microbiota analysis showed that PMP treatment was associated with decreased relative abundance of *Staphylococcus* and increased relative abundance of *Turicibacter*. In addition, PMP significantly restored the mRNA and protein expression of ZO-1, Occludin and Claudin-3 ($P< 0.05$), indicating improved intestinal barrier integrity. PMP also reduced the mRNA expression of *PI3K*, *AKT* and *STAT1* to different extents（$P< 0.05$. These results indicate that PMP alleviated Salmonella spp.-induced enteritis in mice, possibly by improving antioxidant status, reducing IL-6, modulating gut microbiota composition, and restoring intestinal barrier-related molecules.

To Cite This Article: Yuai Y, Miao H, Jiayi L, Kang W, Alghamdi RA, Momenah MA, Mostafa YS and Yongke S, 2026. the efficacy and mechanism of *Prunus mume* ethanol extract in preventing and treating *Salmonella spp* infection in mice. Pak Vet J, 46(5): 1293-1303. http://dx.doi.org/10.29261/pakvetj/2026.116

INTRODUCTION

Bacterial diarrhea is a common and serious disease in livestock and poultry, mainly caused by pathogens such as *Escherichia coli*, Salmonella spp. and *Clostridium perfringens* (Ross *et al*., 2021; Mehdizadeh Gohari *et al*., 2021). These pathogens are typically transmitted through contaminated feed or water and can induce intestinal injury by disrupting microbial homeostasis and triggering inflammatory responses (Rogers *et al*., 2021). In addition to impairing nutrient absorption and growth performance, bacterial diarrhea increases culling and mortality rates, causing substantial economic losses to the livestock industry. Although antibiotics remain the main approach for clinical control, their long-term and irrational use has led to increasing antimicrobial resistance and residue-related food safety concerns (Larsson and Flach, 2022; Siddique *et al*., 2024). Therefore, the development of safe and effective alternatives, particularly natural products from traditional Chinese medicine, has attracted growing attention in veterinary medicine and animal production (Su *et al*., 2020; Millar *et al*., 2021).

Recent studies have shown that gut microbiota dysbiosis plays a central role in the development of enteritis. This dysbiosis is commonly characterized by reduced microbial diversity, depletion of beneficial

commensals, and expansion of inflammation-associated bacteria, thereby contributing to mucosal inflammation and intestinal injury (Aggeletopoulou *et al*., 2019; Qiu *et al*., 2022). Because gut microbiota is closely linked to intestinal barrier integrity, restoration of microbial homeostasis has become an important strategy for preventing and controlling enteric disease. Tight junction proteins, including ZO-1, Occludin, and Claudin-3, are essential for maintaining epithelial integrity and limiting pathogen translocation, whereas persistent dysbiosis and inflammation may disrupt tight junction structure, increase intestinal permeability, and further aggravate intestinal damage (Xie *et al*., 2025). In addition, inflammation-related signaling pathways such as PI3K/AKT and JAK/STAT have been implicated in intestinal inflammatory regulation, epithelial permeability, and mucosal barrier responses during enteric injury. However, available evidence suggests that these pathways act in a context-dependent manner and may reflect host adaptive or pathological responses depending on the disease model, cell type, and stage of injury. Therefore, in the present study, PI3K/AKT- and JAK/STAT-related genes were included only as exploratory pathway-associated indicators, whereas the primary focus remained on gut microbiota disturbance and intestinal barrier-related injury (Zarneshan *et al*., 2020; Lei *et al*., 2021; Qi *et al*., 2023; Asaad and Mostafa, 2024; Akagha *et al*., 2026).

Prunus mume (Wumei in China), the dried near-ripe fruit of Prunus species in the Rosaceae family, is a traditional medicine-food homologous material with long-standing applications in gastrointestinal disorders (Gong *et al*., 2021; Wang *et al*., 2024). In traditional Chinese medicine, it is commonly used to astringe the intestine and relieve diarrhea. Among its bioactive constituents, polysaccharides have received increasing attention because of their potential to regulate gut microbiota, reduce inflammatory responses, and promote intestinal barrier repair (Balasubramaniyam *et al*., 2025; Gao *et al*., 2025; Yang *et al*., 2025). However, the protective effects of *Prunus mume* polysaccharides (PMP) against bacterial enteritis and their relationship with gut microbiota homeostasis remain unclear. Therefore, this study aimed to investigate whether PMP could alleviate Salmonella-induced intestinal injury by modulating gut microbiota composition, improving barrier-related molecules, and attenuating inflammatory and oxidative stress responses. Changes in PI3K/AKT and JAK/STAT-related genes were included only as exploratory indicators associated with inflammatory regulation. This study may provide an experimental basis for the development of PMP as a natural intervention for the prevention and control of bacterial enteritis in livestock and poultry.

MATERIALS AND METHODS

Preparation of *Prunus mume* polysaccharides: Dried *Prunus mume* was purchased from Anhui Shenao Traditional Chinese Medicine Pharmacy (Anhui, China), pulverized, and passed through a 40-mesh sieve. Crude polysaccharides from *Prunus mume* were prepared using a hot water extraction–ethanol precipitation method. Briefly, the pretreated powder was extracted with 8 volumes of distilled water under hot water conditions. The extract was filtered to remove insoluble impurities, and the supernatant was collected and concentrated appropriately. Absolute ethanol was then slowly added to the concentrated extract to a final concentration of 80% (v/v), followed by thorough mixing and incubation at low temperature to allow complete polysaccharide precipitation. The precipitate was collected by centrifugation at 4000 r/min for 10min. Deproteinization was subsequently performed using the Sevag method: Sevag reagent was added to the polysaccharide solution, vigorously mixed, and centrifuged for phase separation, after which the protein layer and organic phase were discarded. This procedure was repeated until proteins were essentially removed. Finally, the deproteinized polysaccharide solution was concentrated and freeze-dried to obtain *Prunus mume* polysaccharides (PMP). The extraction yield of PMP was 9.45% and the total carbohydrate content was 80.06±0.34%. PMP used in the present study represented a crude polysaccharide fraction. Physicochemical characterization, such as FTIR, HPLC profiling, and molecular weight distribution analysis, was not included in the present study.

Animal experiments: Twenty-four 4-week-old ICR mice weighed 18±2g. Equal numbers of both sexes were used. Animals were housed under specific-pathogen-free (SPF) conditions at the Experimental Animal Center of Yangzhou University on metal cages with hardwood bedding under the following conditions: room temperature 23–25°C, relative humidity 45–55%, a 12 h light–dark cycle and animals were allowed adapt to and recover for 3 days before use. The animals were randomly divided into three groups, i.e., control (CD), model (MD) and PMP treatment (TD), with 8 mice in each group.

The TD group received PMP by oral gavage (100mg/kg BW; 10mg/mL) once daily for 14 days, while CD and MD groups received an equal volume of saline. On day 14, bacterial enteritis was induced in the MD and TD groups via intraperitoneal injection of the standard strain Salmonella enterica subsp. enterica ATCC 9150 (1×10^7 CFU/kg), whereas the CD group received sterile saline. Clinical signs were recorded 24 h post-challenge. Blood samples were collected via the retro-orbital plexus under light anesthesia, followed by euthanasia. Major organs and intestinal segments were harvested for subsequent analyses, and organ indices were calculated.

Analysis of intestinal bacterial load: Segments of duodenum, jejunum, and ileum were excised under sterile conditions, weighed (0.1g), and homogenized in sterile saline. After dilution plating on Luria–Bertani agar, cultures were incubated at 37°C for 12h and counts of CFU/g tissue determined. All experiments were performed with biological replicates of n≥3 and the exact number of biological replicates for each assay is indicated in the corresponding figure legends.

Histopathological examination of intestinal tissues: Jejunal and ileal tissues were fixed in 4% paraformaldehyde, paraffin-embedded, sectioned (4–5μM), and stained with hematoxylin and eosin. Histopathological changes were examined under a light

microscope. Intestinal mucosal injury was quantitatively evaluated by measuring villus height, crypt depth, and the villus height/crypt depth (V/C) ratio.

Detection of serum antioxidant and inflammatory markers: Serum samples were centrifuged at 4,200×g for 15min and stored at −20°C. The levels of SOD, T-AOC, MDA, and GSH-Px were measured using commercial assay kits (BC5165, BC1315, BC6415, and BC1195, respectively; Solarbio, Beijing, China). Serum cytokines, including IL-6, IL-10 and TNF-α, were determined using commercial ELISA kits (RM17709, RM17935, and RM17776, respectively; ABclonal, Wuhan, China), according to the manufacturers' instructions.

RT-qPCR and Western blot analyses: Colon tissues were rinsed with ice-cold saline, snap-frozen in liquid nitrogen, and stored at −80°C. Total RNA was extracted from 30–50mg of colon tissue using TRIzol reagent, and equal amounts of RNA were reverse-transcribed into cDNA. RT-qPCR was performed using the primers listed in Table 1 and SYBR Green qPCR Master Mix on a real-time PCR system to determine the mRNA expression levels of ZO-1, Occludin, Claudin-3, PI3K, AKT and STAT1. Primer specificity and amplification efficiency were verified before formal qPCR analysis to ensure the accuracy of gene expression results. GAPDH was used as the internal control, and relative expression was calculated using the $2^{-\Delta\Delta Ct}$ method.

Table1: Primer Sequences for Mouse Quantitative Real-Time PCR

Gene Name	Primer direction	Primer Sequence (5'→3')
m-β-actin	Forward	TTGCAGCTCCTTCGTTGCC
	Reverse	GACCCATTCCCACCATCACA
m-Akt	Forward	CCTGGTGGTCATGGAGAACT
	Reverse	CTTCAGCCCTTTGCTCAGTG
m-PI3K	Forward	AGTGGCTGAAACGGACCTAT
	Reverse	TCCAGGCTGTCATGTTTTGC
m-STAT1	Forward	GGAAAAGCAAGACTGGGAGC
	Reverse	TCCAGAGAAAAGCGGCTGTA
m-ZO-1	Forward	GTTGGTACGGTGCCCTGAAAGA
	Reverse	GCTGACAGGTAGGACAGACGAT
m-Occludin	Forward	AGCTTCCATTAACTTCGCCTGTG
	Reverse	TCGCCGCCAGTTGTGTAGTC
m-Claudin-3	Forward	TCATCGTGGTGTCCATCCTGCT
	Reverse	AGAGCCGCCAACAGGAAAAGCA

For Western blot analysis, whole colon tissues were homogenized in ice-cold RIPA lysis buffer containing protease inhibitors, clarified at 12,000×g for 15 min at 4°C, and quantified by BCA assay. Samples containing equivalent amounts of protein were separated by SDS-PAGE and transferred to PVDF membranes. Membranes were blocked in 5% non-fat milk for 1h before overnight incubation with ZO-1, Occludin, Claudin-3 or β-actin antibodies at 4°C followed by incubation with HRP-conjugated secondary antibodies for 1h at room temperature. Bands were visualized using an ECL detection system and quantified by ImageJ. Protein expression levels were normalized to β-actin.

Analysis of gut microbiota diversity: Total genomic DNA was extracted from rectal samples (n=6 per group) using the OMEGA soil for community profiling, the total genomic DNA isolated from individual rectal swabs of six mice per group was used. Total genomic DNA was extracted using OMEGA Soil DNA Kit (OMEGA Bio-Technik) and assessed using a NanoDrop NC2000 spectrophotometer for quality and concentration. The V3–V4 regions of the bacterial 16S rRNA gene were amplified using the primers 338F (5'-ACTCCTACGGG AGGCAGCA-3') and 806R (5'-GGACTACHVGGG TWTCTAAT-3'). Amplification reactions were performed in a 25μL reaction system containing FastPfu DNA Polymerase under the following conditions: initial denaturation at 98°C for 5 min, followed by 25 cycles of 98°C for 30s, 53°C for 30s and 72°C for 45s, with a final extension at 72°C for 5 min. Purified amplicons were quantified, pooled in equimolar concentrations and sequenced on an Illumina MiSeq platform.

Raw reads were quality-filtered and processed using DADA2 in QIIME2 for the generation of amplicon sequence variants (ASVs). Taxonomic assignment was conducted by using a pre-trained classifier. Microbial community composition was analyzed based on relative abundance at different taxonomic levels. Alpha and beta diversity were assessed, with beta diversity visualized by Principal Coordinate Analysis (PCoA). LEfSe analysis was applied to identify differentially abundant taxa and potential microbial biomarkers among groups. Functional prediction based on 16S rRNA sequencing data was conducted with KEGG and MetaCyc databases.

Statistical analysis: The software programs GraphPad Prism (v10.4.1) and SPSS (v26.0) were adopted. Analysis of variance (ANOVA) and t-test were applied. Results were expressed as mean ± SEM. Significant level was set to $P<0.05$. There was no significant difference in the body weight of mice before infection with S. spp. ($P>0.05$).

RESULTS

Effects of PMEE on mouse body weight: No significant difference in baseline body weight was observed among the groups before Salmonella spp. infection ($P>0.05$). After infection, the body weight of mice in the MD group decreased significantly compared with that in the CD group ($P<0.05$), whereas body weight loss in the TD group was less pronounced than that in the MD group (Fig. 1A). These results indicate that PMP alleviated infection-associated weight loss in mice.

Effects of PMP on intestinal bacterial load and organ indices in S. spp-infected mice: Analysis of intestinal bacterial load showed that PMP treatment reduced bacterial burden in the intestinal tissues of infected mice. Specifically, bacterial counts in the duodenum ($P<0.01$), jejunum ($P<0.0001$) and ileum ($P<0.01$) were significantly lower in the TD group than in the MD group (Fig. 1B). To further evaluate the systemic effects of infection, organ indices were analyzed. The spleen index was significantly increased in the MD group compared with the CD group ($P<0.01$). Although the lung and liver indices did not show statistically significant differences, an increasing trend was observed in the MD group. Following PMP treatment, the spleen and lung indices in the TD group were reduced relative to the MD group and were closer to those in the CD group, suggesting partial alleviation of infection-associated organ enlargement (Fig. 1C).

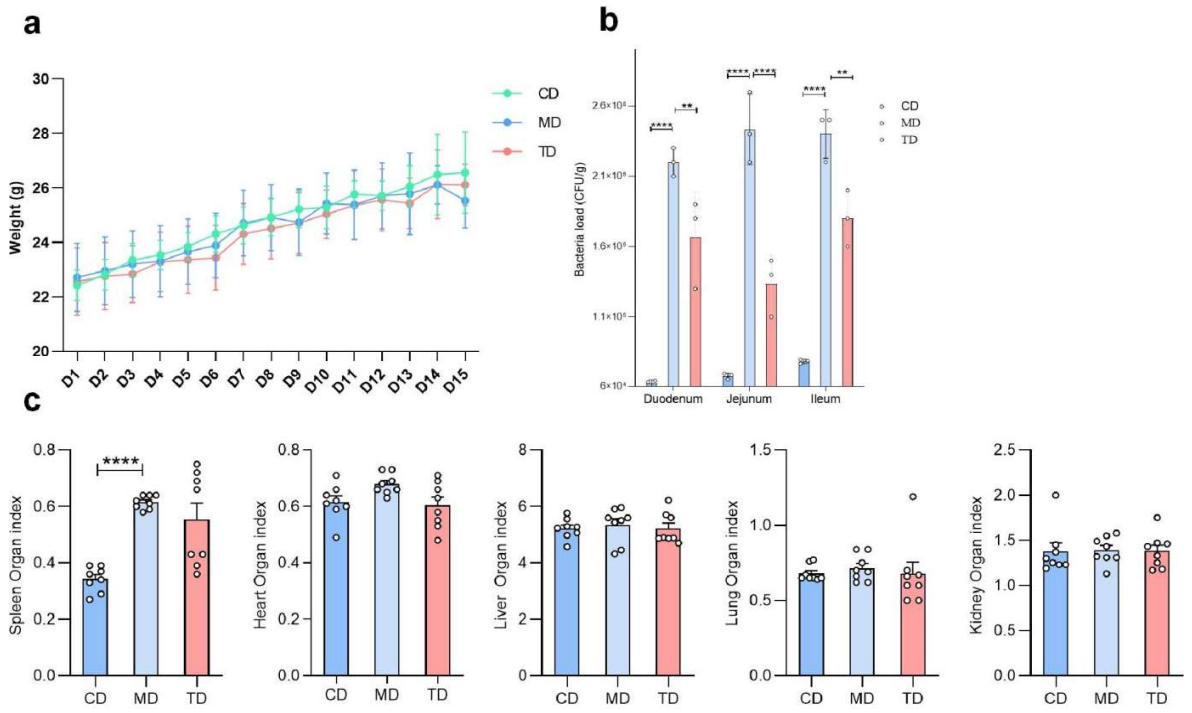

Fig. 1: PMEE rescued intestinal damages in mice induced by LPS. (A) body weights, (B) Bacterial loads (C) Organ index Statistica. significance is indicated as *P<0.05; **P<0.01; ***P< 0.001; ****P<0.0001. Data are presented as mean± SEM (n=8).

Effects of PMP on *S. spp*-induced intestinal injury in mice: Histopathological examination revealed obvious intestinal injury in the MD group, characterized by epithelial shedding, villus damage, and crypt disorder. In contrast, these pathological changes were alleviated in the TD group (Fig. 2). Quantitative analysis further showed that, in the jejunum, villus height was significantly reduced (P<0.01), crypt depth was significantly increased (P<0.0001) and the villus height/crypt depth (V/C) ratio was significantly decreased (P<0.0001) in the MD group compared with the CD group. Compared with the MD group, PMP treatment significantly increased villus height (P<0.01), decreased crypt depth (P<0.01) and increased the V/C ratio (P<0.001). In the ileum, villus height was significantly reduced (P<0.05), crypt depth was significantly increased (P<0.01) and the V/C ratio was significantly decreased (P<0.01) in the MD group compared with the CD group. Compared with the MD group, villus height was significantly increased in the TD group (P<0.05), whereas crypt depth and the V/C ratio did not differ significantly. These results indicate that PMP alleviated Salmonella spp.-induced intestinal histomorphological injury, with a more pronounced improvement in the jejunum.

Effects of PMP on oxidative stress and inflammatory responses in mice: Compared with the MD group, PMP treatment significantly increased serum T-AOC (P<0.01), SOD (P<0.05), and GSH-Px (P<0.001) and significantly decreased IL-6 levels (P<0.0001). MDA and TNF-α levels in the TD group also showed a downward trend, although the differences were not statistically significant. These findings indicate that PMP improved selected antioxidant and inflammatory indices in Salmonella-infected mice.

Effects of PMP on *S. spp-induced* gut microbiota composition in mice: Sequencing analysis showed that the CD, MD, and TD groups generated more than 89,000, 62,000, and 84,000 raw reads, respectively, and that at least 69,000, 52,000, and 70,000 high-quality reads were retained after denoising and filtering, indicating sufficient sequencing quality for downstream analysis (Table 2). Good's coverage values ranged from 0.9922 to 0.9999, indicating adequate coverage of the overall bacterial community structure (Table 2). Alpha diversity analysis showed that the CD group exhibited the highest microbial richness and diversity, followed by the TD group, whereas the MD group showed the lowest values based on the Chao1 and Shannon indices, suggesting a trend toward reduced microbial richness and diversity after Salmonella spp. infection, which was partially improved after PMP treatment (Table 3; Fig. 4A). In addition, the MD group showed a wider distribution range in Pielou's evenness and observed species indices than the CD and TD groups, indicating greater inter-sample heterogeneity (Pielou, 1966). Rarefaction curves approached saturation in all samples, suggesting that the sequencing depth was sufficient for the subsequent analyses, while rank-abundance curves showed the expected distribution pattern of dominant and low-abundance taxa (Fig. 4B, C). Beta diversity analysis based on PCoA further revealed distinct clustering tendencies among the CD, MD, and TD groups, indicating differences in microbial community composition among groups (Fig. 4D).

At the taxonomic level, PMP treatment was associated with altered microbial composition in infected mice (Figs. 5–7). Compared with the MD group, the TD group showed a decreased relative abundance of Staphylococcus and an increased relative abundance of *Turicibacter*. Overall, these results suggest that PMP partially modulated the intestinal microbial community disturbed by Salmonella spp. infection.

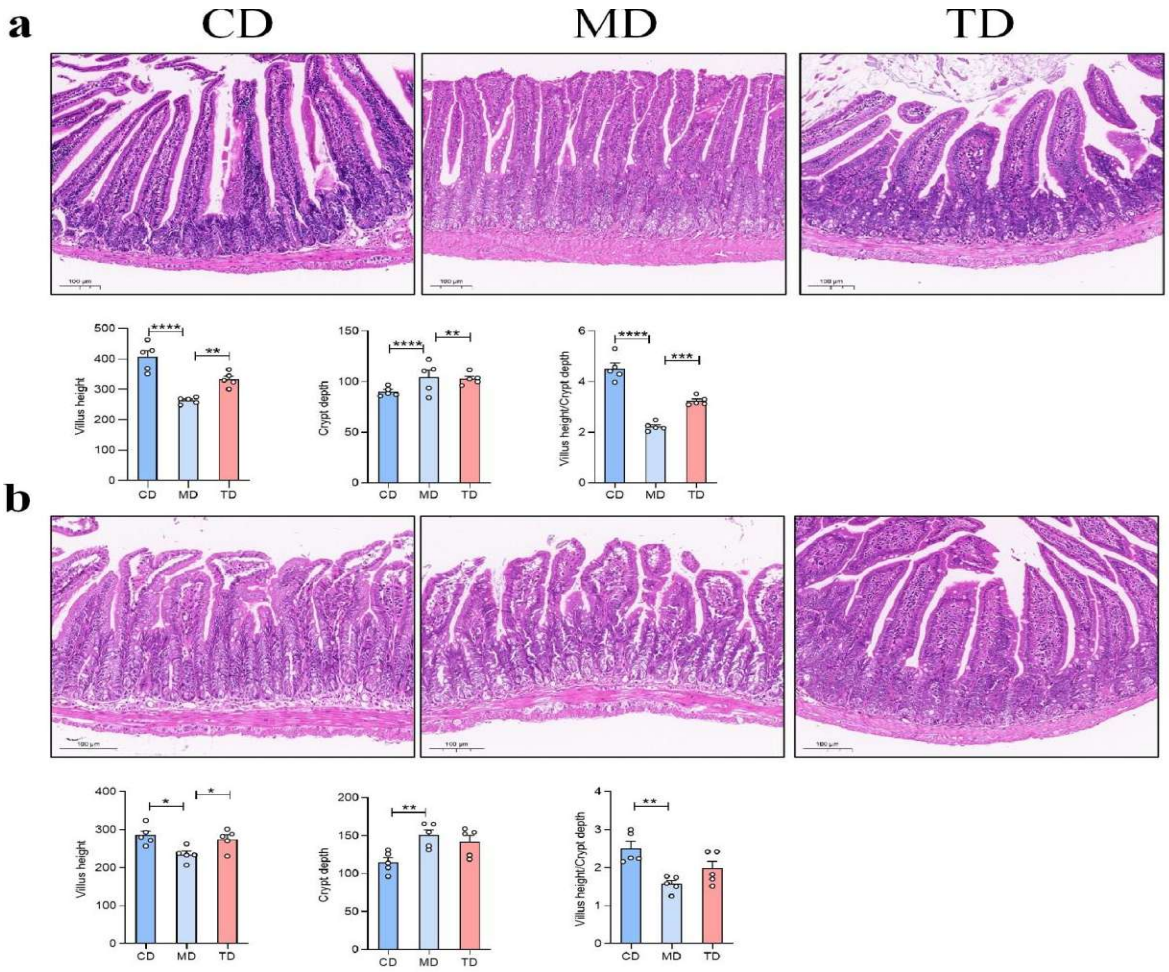

Fig. 2: Pathological analysis of (A) the jejunum, and(B) the ileum. Scale bar 100 μm. significance is indicated as *P<0.05; **P<0.01; ***P< 0.001; ****P<0.0001 Data are presented as mean ± SEM (n=5).

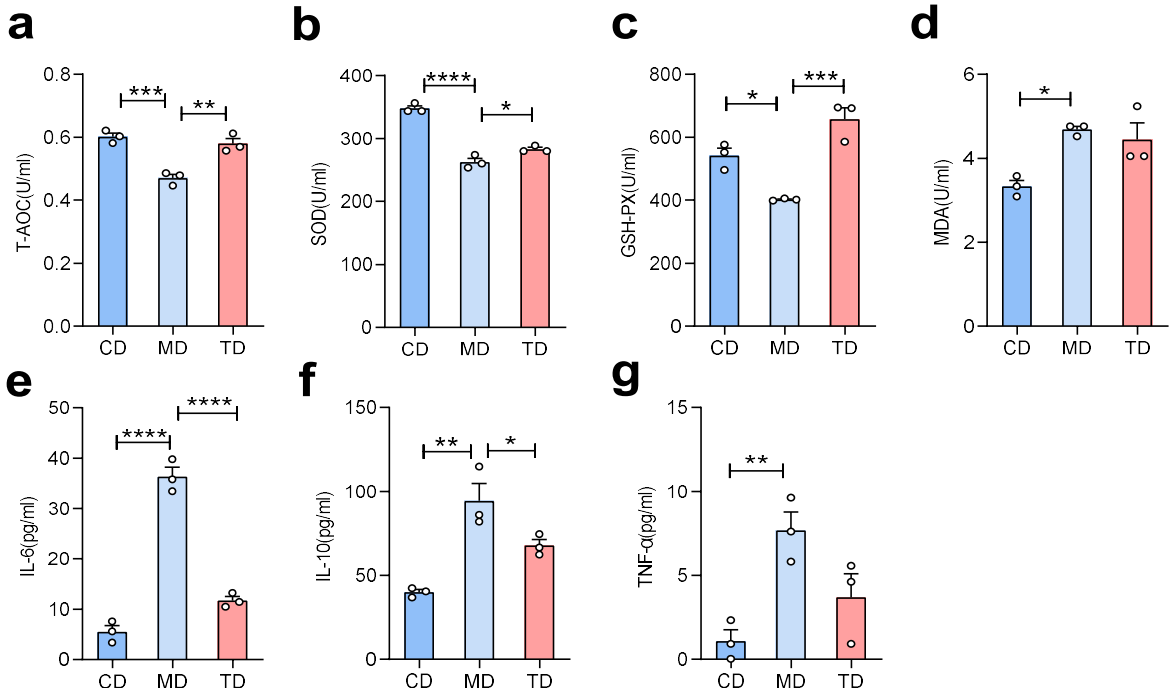

Fig. 3: PMP-mediated serum oxidation resistance and inflammation levels (A) T-AOC, (B) SOD, (C) GSH-Px, (D) MDA, (E) IL-6, (F) IL-10, (G) TNF-α. significance is indicated as *P<0.05; **P<0.01; ***P< 0.001; ****P<0.0001 ; data are presented as the mean±SEM (n=3).

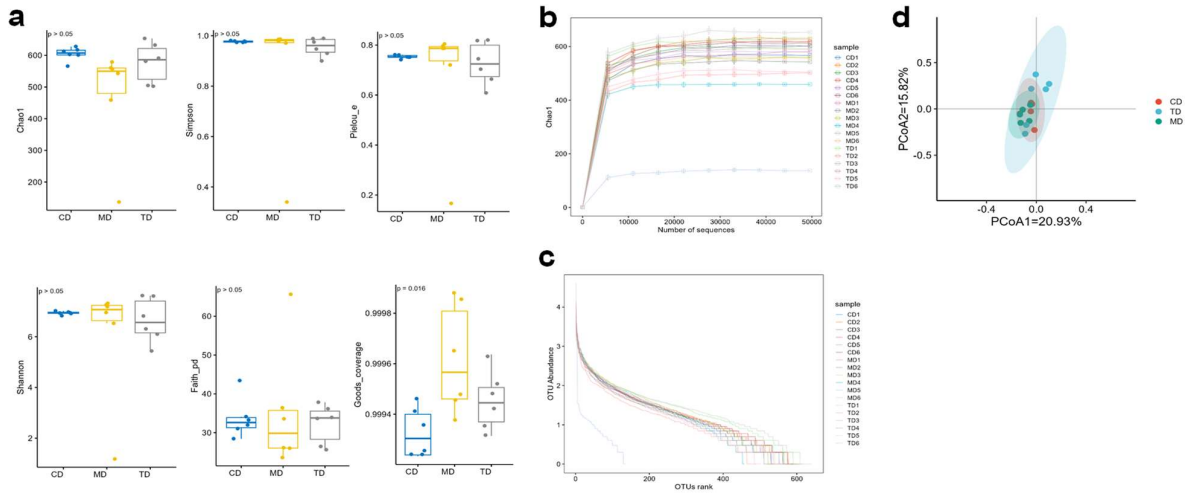

Fig. 4: Alpha and beta diversity analysis (n=6). (a) Diversity indexes, (b) Rarefaction curve (c) Rank abundance curve, (d) Principal coordinate analysis (PCoA).

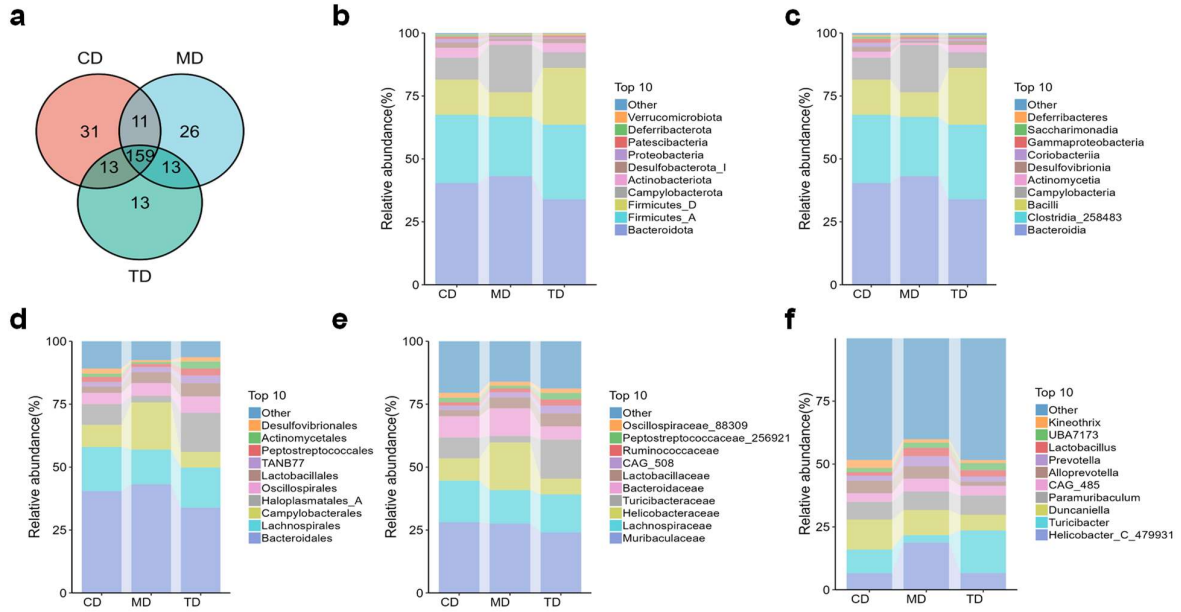

Fig. 5: Venn diagram of ASVs and PPEM-mediated changes in the intestinal microbiota of S. sppinduced mice in different taxa (n=6). (a) Venn diagram of ASVs,(b) Phylum,(c) Class, (d) Order, (e) Family, (f) Genus.

Table 2: Quality filtering statistics of microbial sequencing data for samples in different treatment groups.

SampleID	Input	Filtered	Denoised	Merged	Non-chimeric	Non-singleton
CD1	89392	81712	80308	73470	69258	69233
CD2	109347	100104	98789	92350	88625	88594
CD3	102114	94516	93480	88285	85110	85096
CD4	104348	95608	94656	90667	87966	87947
CD5	103775	93577	92534	87433	84115	84089
CD6	102568	93227	91929	85430	80340	80311
MD1	97823	89813	89104	85943	84751	84741
MD2	102322	94243	93303	87501	80431	80401
MD3	100963	92826	91877	86662	83903	83885
MD4	61965	56070	55542	52969	52193	52179
MD5	76123	69288	68884	68385	67723	67723
MD6	91209	83112	82407	79595	78384	78373
TD1	107525	98331	97346	92464	89990	89976
TD2	83653	75589	74815	71756	69492	69465
TD3	111412	100412	98938	91561	86836	86810
TD4	94105	85811	85005	82252	80922	80912
TD5	90082	81592	80632	76601	73414	73402
TD6	93605	86055	85017	79198	76867	76846

Functional prediction based on 16S rRNA sequencing suggested differences in microbial functional profiles among groups (Fig. 8). In the MD group, pathways related to lipopolysaccharide biosynthesis, peroxisome, and apoptosis were enriched, whereas the TD group showed enrichment of pathways such as starch and sucrose metabolism and ABC transporters. MetaCyc analysis also showed distinct pathway distributions among groups. Taken together, these findings indicate that PMP partially reshaped the gut microbial community in Salmonella spp.-infected mice and was associated with predicted functional shifts in the microbiota.

PMP ameliorated intestinal mucosal barrier injury and modulated the expression of PI3K/AKT/STAT1-related genes: As shown in Fig. 9, compared with the CD group, the mRNA expression levels of ZO-1, Occludin, and Claudin-3 in colon tissues were decreased in the MD

Table 3: Statistical Table of Alpha Diversity Indices for Microbial Sequencing Samples

Sample	Chao1	Faith_pd	Goods_coverage	Observed_species	Pielou	Shannon	Simpson
CD1	566.12	31.06586957	0.999414969	558	0.760598969	6.939797261	0.979091033
CD2	627.5192308	34.09894065	0.999233407	614	0.752919889	6.973615425	0.973818446
CD3	602.3225806	43.40901443	0.999455316	591	0.741580544	6.827742686	0.97379818
CD4	617.2727273	31.94841958	0.999354448	606	0.751664047	6.947761567	0.978432568
CD5	600.8076923	33.277079	0.999253581	588	0.751894937	6.917187057	0.976411115
CD6	612.2641509	28.41306031	0.999233407	599	0.761214931	7.023282725	0.981024746
MD1	578.8846154	26.1144042	0.999374622	561	0.787158605	7.18821979	0.984157883
MD2	542.6326531	25.9905626	0.999475489	536	0.720418914	6.531382132	0.970931009
MD3	557	33.57582869	0.999455316	548	0.804590367	7.320188976	0.986605618
MD4	458.7894737	23.57070012	0.999878959	458	0.786967632	6.956167278	0.978317427
MD5	137.2352941	65.67506955	0.999858786	136	0.16649226	1.180007706	0.340359233
MD6	560.8571429	36.45723123	0.999657051	556	0.796148923	7.260035111	0.985964665
TD1	632	36.12459293	0.999414969	618	0.820254476	7.604959051	0.989439767
TD2	502.037037	25.58156829	0.999475489	490	0.60851254	5.438056252	0.90018572
TD3	581.1956522	37.83024785	0.999314101	569	0.744989186	6.818353234	0.975084278
TD4	590.75	33.90417605	0.999515836	585	0.663872074	6.102506499	0.930445512
TD5	505.4772727	26.49709244	0.999636877	502	0.703776085	6.313957798	0.94752095

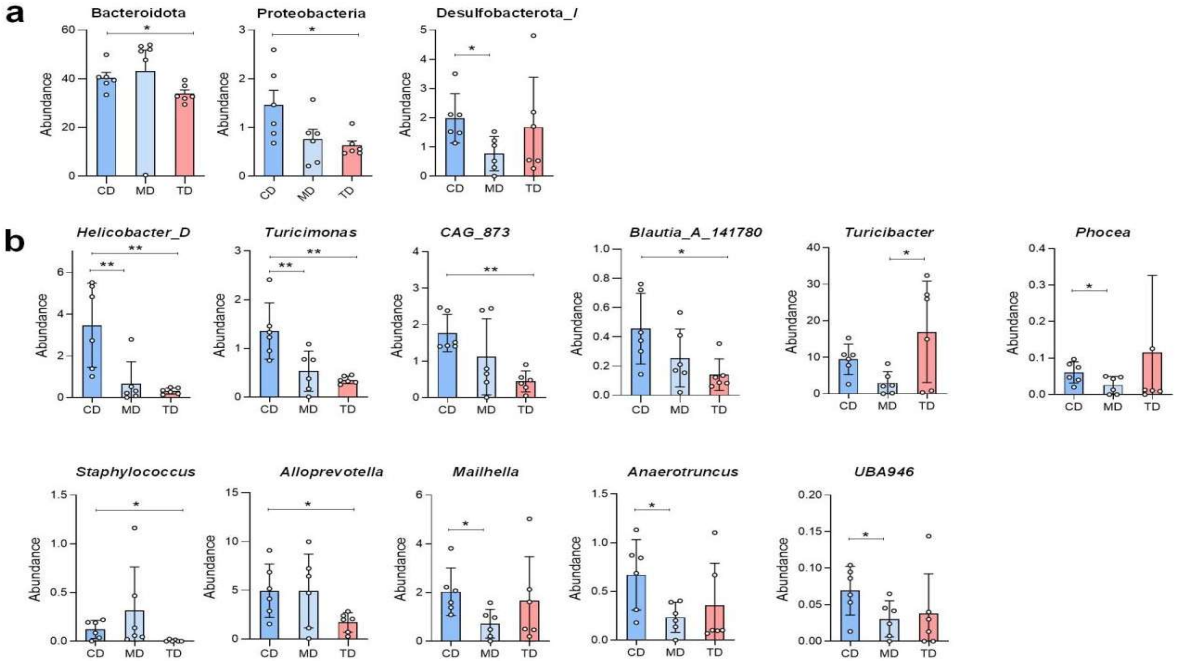

Fig. 6: Revealing microbiota differences in mice in different groups using ANOVA analysis. (A) phyla, (B) genus. Significance is presented as *P<0.05, **P<0.01 and ***P<0.001; data are presented as the mean ± SEM (n=6).

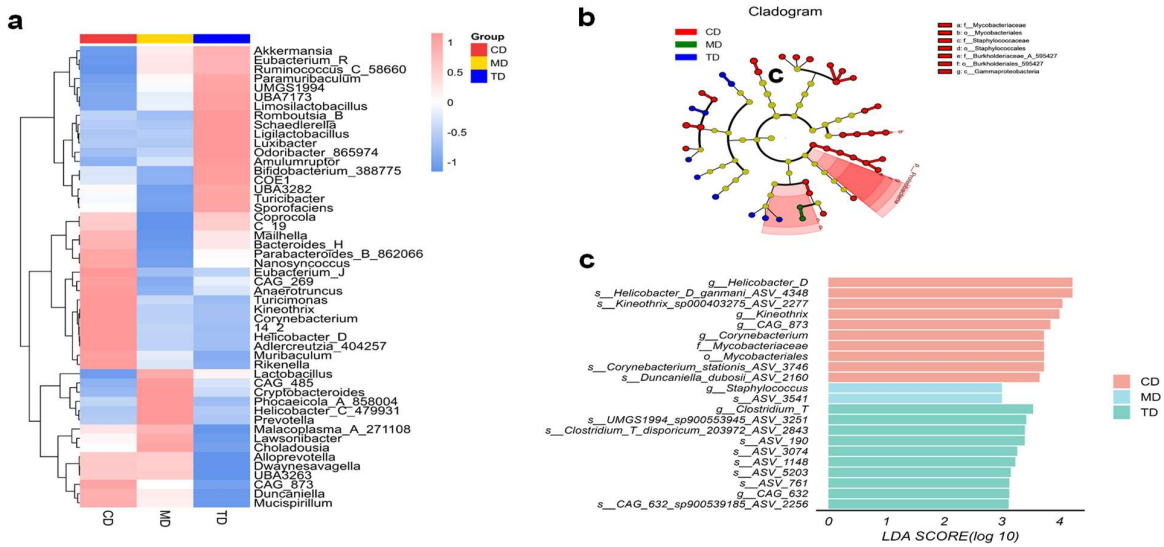

Fig. 7: Heatmap and LEfSe analysis of mice microbiota in different groups (n=6). (A) Heatmap. (B,C) LEfSe.

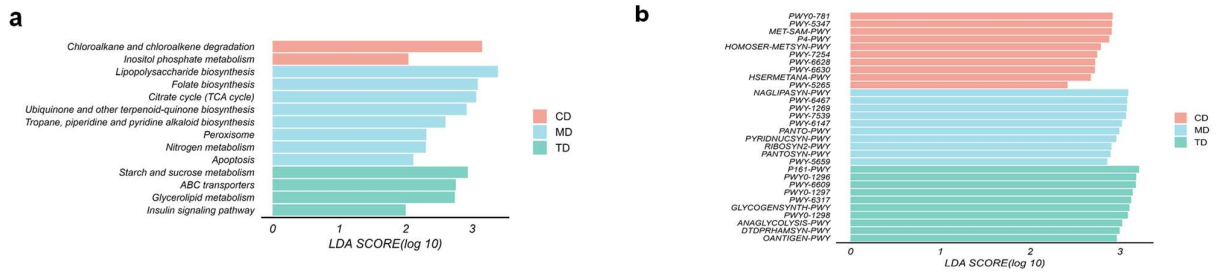

Fig. 8: Functional analysis of mice microbiota (a) KEGG pathway analysis and (b) MetaCyc pathway analysis (n=6).

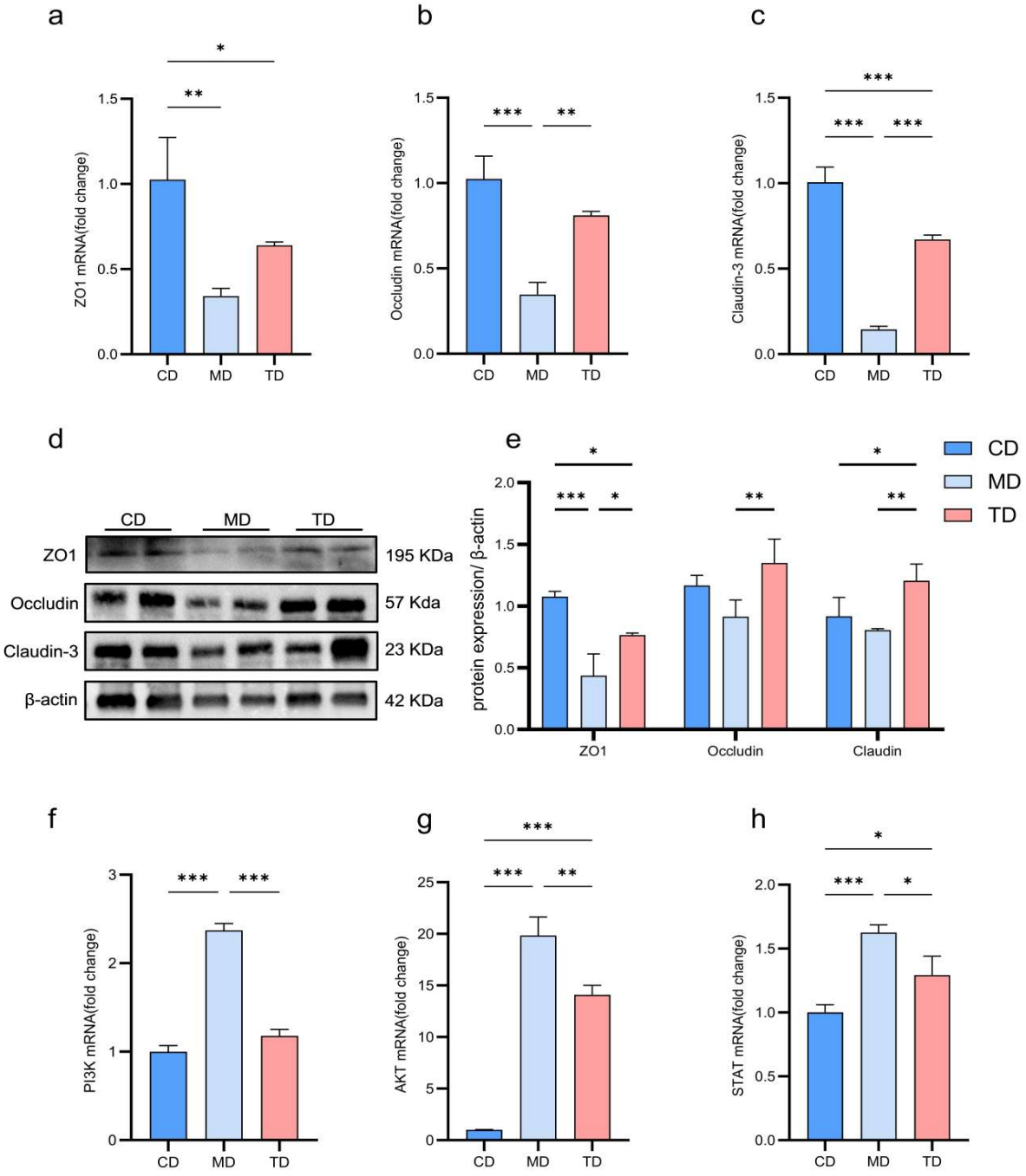

Fig. 9: PMP ameliorated intestinal mucosal barrier injury and modulated the expression of PI3K/AKT/STAT1-related genes in mice with *S. spp*-induced enteritis (n=3). (a-c) Relative mRNA expression levels of ZO-1, Occludin and Claudin-3 in colon tissues were determined by RT-qPCR. (d) Representative Western blot bands of ZO-1, Occludin, Claudin-3 and β-actin in colon tissues. (e) Densitometric analysis of ZO-1, Occludin and Claudin-3 protein expression normalized to β-actin. (f-h) Relative mRNA expression levels of PI3K, AKT and STAT1 in colon tissues were determined by RT-qPCR. Data are presented as mean ± SD. P<0.05, P<0.01, P<0.001.

group, indicating impairment of intestinal barrier-related molecules in the model mice. Among them, Occludin and Claudin-3 mRNA expression levels were significantly restored after PMP treatment compared with the MD group ($P<0.01$ and $P<0.001$, respectively), whereas ZO-1 mRNA showed an increasing trend after PMP treatment but did not differ significantly from that in the MD group. Western blot analysis showed that the protein expression levels of ZO-1, Occludin, and Claudin-3 were reduced in the MD group, while PMP treatment partially restored their expression, particularly for ZO-1 and Claudin-3.

The mRNA expression levels of PI3K, AKT, and STAT1 were significantly increased in the MD group compared with the CD group. After PMP treatment, the expression levels of these genes were reduced to different extents, with PI3K showing the most pronounced decrease, followed by AKT and STAT1. In particular, PI3K, AKT, and STAT1 mRNA expression levels were significantly lower in the TD group than in the MD group ($P<0.001$, $P<0.01$ and $P<0.05$, respectively). However, because these signaling molecules were assessed only at the mRNA level, the present results indicate only that PMP treatment was associated with altered PI3K/AKT/STAT1-related gene expression rather than direct pathway modulation.

DISCUSSION

Salmonella spp. infection caused obvious body weight loss, increased spleen index and intestinal injury in mice, indicating successful establishment of the enteritis model. As reported previously, enteric infection–associated anorexia, malabsorption, and dehydration are important contributors to weight loss during acute intestinal disease (Ledwaba *et al*., 2020). In the present study, PMP treatment alleviated body weight loss and reduced intestinal bacterial burden and splenomegaly. Since increased spleen index is commonly associated with systemic inflammatory stress during Salmonella infection (Zhang *et al*., 2020), the reduction observed after PMP treatment may reflect partial attenuation of infection-related systemic injury. However, the decreased bacterial load observed in intestinal tissues should still be interpreted cautiously, as it reflects an in vivo protective effect rather than direct evidence of antibacterial activity.

Histopathological analysis further supported the protective effect of PMP on intestinal injury. The MD group showed epithelial damage, villus shortening, and crypt disorder, whereas these lesions were alleviated after PMP treatment. Intestinal morphology is closely related to mucosal function, and the villus height/crypt depth (V/C) ratio is widely used as an indicator of absorptive and epithelial renewal status (Jha and Mishra, 2021). In the present study, PMP significantly improved jejunal villus height, crypt depth, and the V/C ratio, while its effect in the ileum was less pronounced. This pattern suggests that PMP contributed to maintaining intestinal morphology, especially in the jejunum. Similar observations have been reported in other enteric injury studies, in which improvement of villus architecture was associated with better mucosal recovery and homeostasis (Yue *et al*., 2020; Troha and Ayres, 2022).

Oxidative stress and inflammatory responses are major features of enteric infection. Excessive reactive oxygen species can disrupt epithelial integrity and aggravate mucosal damage, as reported by Ikeda *et al*. (2018). In the present study, PMP increased serum SOD, GSH-Px and T-AOC, suggesting improvement in selected antioxidant indices. Because SOD and GSH-Px are key antioxidant enzymes, their increase may indicate enhanced endogenous antioxidant defense, which is often linked to maintenance of intestinal barrier function (Wen *et al*., 2019). Inflammatory signaling is also closely connected with oxidative stress, and ROS accumulation can promote inflammatory cascades such as NF-κB activation (Ray *et al*., 2012; Liu *et al*., 2017). Here, PMP reduced IL-6, suggesting partial attenuation of inflammation. However, MDA and TNF-α were not significantly changed, indicating that the protective effect of PMP was not consistent across all measured indices.

Gut microbiota analysis showed that Salmonella spp. infection was associated with reduced microbial richness and altered community structure, whereas PMP partially improved these changes. At the taxonomic level, PMP treatment was mainly associated with decreased Staphylococcus and increased Turicibacter. Because Staphylococcus includes opportunistic pathogens and has been linked to intestinal dysbiosis and pathogenicity (Idrees *et al*., 2021), its reduction may reflect partial correction of infection-related microbial disturbance. By contrast, enrichment of Turicibacter has been associated with a healthier intestinal microbial environment in recent microbiota-related studies (Dong *et al*., 2024). Overall, the present results suggest that PMP may help re-establish a more balanced microbial community, which is in line with the broader view that gut microbial recovery is important for intestinal health maintenance (Sasidharan Pillai *et al*., 2024). Functional prediction also indicated differences among groups. In the MD group, pathways related to lipopolysaccharide biosynthesis, peroxisome, and apoptosis were enriched, whereas the TD group showed relative enrichment of starch and sucrose metabolism and ABC transporters. Since lipopolysaccharide is closely associated with inflammatory stimulation (Rietschel and Westphal, 2020), and ABC transporters are relevant to bacterial transport functions (Fath and Kolter, 1993), these predicted changes may reflect altered microbial functional tendencies during infection and recovery. Nevertheless, because these results were inferred from 16S rRNA sequencing rather than direct metabolomic analysis, they should be interpreted cautiously (Virzì *et al*., 2022).

The intestinal barrier is essential for limiting pathogen translocation and maintaining mucosal homeostasis. Tight junction-related molecules such as ZO-1, Occludin, and Claudin-3 are key structural components of this barrier (Di Sabatino *et al*., 2023). In this study, the expression of ZO-1, Occludin, and Claudin-3 was reduced in the MD group and partially restored after PMP treatment, supporting an association between PMP intervention and improvement of barrier-related molecules. This finding is also consistent with previous reports showing that intestinal inflammation is often accompanied by disruption of tight junction structure and increased epithelial permeability (Wang *et al*., 2022; Zhao *et al*., 2022). In addition, PI3K, AKT, and STAT1 mRNA expression levels were elevated in the MD group and

decreased after PMP treatment. Since PI3K/AKT signaling has been implicated in intestinal inflammation and barrier injury in other studies (Li *et al*., 2022; Zhang *et al*., 2025), and STAT1 is also involved in cytokine-related inflammatory regulation (Wang *et al*., 2024), these results suggest that PMP treatment was associated with altered inflammation-related gene expression. However, because these signaling molecules were assessed only at the transcript level, the present findings indicate altered gene expression associated with PMP treatment rather than direct pathway modulation.

This study has several limitations. PMP was used as a crude polysaccharide fraction without further structural characterization. Microbiota-related functional changes were predicted from 16S rRNA data rather than validated by metabolomics or metagenomics. In addition, PI3K/AKT/STAT1 was evaluated only at the mRNA level. Despite these limitations, the present findings support a protective effect of PMP against Salmonella spp.-induced enteritis and provide a basis for further investigation of its active components and underlying mechanisms.

Conclusions: In conclusion, PMP alleviated Salmonella spp.-induced enteritis in mice, as shown by reduced body weight loss, splenomegaly, intestinal bacterial burden, and mucosal injury. PMP was also associated with improved antioxidant indices, reduced IL-6, partial restoration of barrier-related molecules, and modulation of gut microbiota. However, PMP was not structurally characterized, microbiota-related functions were predicted from 16S rRNA data, and PI3K/AKT/STAT1 was assessed only at the mRNA level. Therefore, PMP should be regarded as a bioactive intervention with potential protective value rather than a confirmed therapeutic candidate, and further validation is needed in livestock and poultry models.

Funding: This work was funded by the National Natural Science Foundation of China (NSFC No. 32160845), Princess Nourah bint Abdulrahman University Researchers Project number (PNURSP2026R224), Princess Nourah bint Abdulrahman University, Riyadh, Saudi Arabia, and the Deanship of Research and Graduate Studies at King Khalid University through a Large Research Project under grant number (R.G.P.2/268/46).

Acknowledgements: The authors acknowledge Princess Nourah bint Abdulrahman University Researchers Supporting Project number (PNURSP2026R224), Princess Nourah bint Abdulrahman University, Riyadh, Saudi Arabia. The authors extend their appreciation to the Deanship of Research and Graduate Studies at King Khalid University for funding this work through a Large Research Project under grant number RGP2/268/46.

Authors contribution: YY MH, JL Conceptualization, Methodology, Investigation, Formal analysis, Writing – Original Draft, Funding acquisition, and Project administration; WK Investigation, Resources, Data Curation, Validation; RA, MM, YM Methodology, Writing – Review; YY and YS Conceptualization, Supervision, Funding acquisition, Project administration, Writing – Review & Editing.

Declaration of Competing Interest: None.

REFERENCES

Aggeletopoulou I, Konstantakis C, Assimakopoulos SF *et al*., 2019. The role of the gut microbiota in the treatment of inflammatory bowel diseases. Microbial Pathogenesis 137:103774.

Akagha MJ, Georgolopoulos G, Martin D, *et al*., 2026. IFNγ shapes macrophage inflammatory responses by STAT1 isoform-specific epigenetic and transcriptional mechanisms. BMC Genomics 27:256.

Asaad GF and Mostafa RE, 2024. Amelioration of acetic acid-induced ulcerative colitis in rats by cetirizine and loratadine via regulation of the PI3K/Akt/Nrf2 signalling pathway and pro-inflammatory cytokine release. Iranian Journal of Basic Medical Science 27:761-767.

Balasubramaniyam T, Ahn HB, Lim J, *et al*., 2025. Therapeutic potential of polysaccharides in inflammation: current insights and future directions. International Immunopharmacology 166:115538.

Chao A, 1984. Nonparametric estimation of the number of classes in a population. Scandinavian Journal of Statistics 11:265-270.

Di Sabatino A, Santacroce G, Rossi CM, *et al*., 2023. Role of mucosal immunity and epithelial-vascular barrier in modulating gut homeostasis. Internal and Emergency Medicine 18:1635-1646.

Dong YJ, Zhang YP, Jiang XF, *et al*., 2024. Beneficial effects of dendrobium officinale national herbal drink on metabolic immune crosstalk via regulate SCFAs-Th17/Treg. Phytomedicine 132:155816.

Fath MJ, Kolter R, 1993. ABC transporters: bacterial exporters. Microbiology Reviews 57:995-1017.

Gao M, Zhang W, Ma Y, *et al*., 2025. Bioactive polysaccharides prevent lipopolysaccharide-induced intestinal inflammation via immunomodulation, antioxidant activity and microbiota regulation. Foods 14:2575.

Gong XP, Tang Y, Song YY, *et al*., 2021. Comprehensive review of phytochemical constituents, pharmacological properties, and clinical applications of *Prunus mume*. Frontiers in Pharmacology 12:679378.

Good IJ, 1958. The population frequency of species and the estimation of the population parameters. Biometrika 40:237-264.

Idrees M, Sawant S, Karodia N, *et al*., 2021. *Staphylococcus aureus* biofilm: morphology, genetics, pathogenesis and treatment strategies. International Journal of Environmental Research and Public Health 18:7602.

Ikeda M, Shimizu K, Ogura H, *et al*., 2018. Hydrogen-rich saline regulates intestinal barrier dysfunction, dysbiosis, and bacterial translocation in a murine model of sepsis. Shock 50:640-647.

Jha R, Mishra P, 2021. Dietary fiber in poultry nutrition and their effects on nutrient utilization, performance, gut health, and on the environment: a review. Journal of Animal Science Biotechnology 12:51.

Jiang QB, Zhang QR, Li XG, *et al*., 2025. Preparation of components and study on pharmacodynamic substances of traditional Chinese medicine *Prunus mume*. Central South Pharmacy 23:305-311.

Larsson DJ, Flach CF, 2022. Antibiotic resistance in the environment. Nature Reviews in Microbiology 20:257-269.

Ledwaba SE, Costa DV, Bolick DT, *et al*., 2020. Enteropathogenic *Escherichia coli* infection induces diarrhea, intestinal damage, metabolic alterations and increased intestinal permeability in a murine model. Frontiers in Cellular and Infectious Microbiology 10:595266.

Lei H, Crawford MS, McCole DF, 2021. JAK-STAT pathway regulation of intestinal permeability: pathogenic roles and therapeutic opportunities in inflammatory bowel disease. Pharmaceuticals (Basel) 14(9):840.

Li C, Wang L, Zhao J, *et al*., 2022. *Lonicera rupicola* Hook.f.et Thoms flavonoids ameliorated dysregulated inflammatory responses, intestinal barrier and gut microbiome in ulcerative colitis via PI3K/AKT pathway. Phytomedicine 104:154284.

Liu T, Zhang L, Joo D, *et al*., 2017. NF-κB signaling in inflammation. Signal Transduction and Target Therapy 2:17023.

Mehdizadeh Gohari I, Navarro MA, Li J, *et al*., 2021. Pathogenicity and virulence of *Clostridium perfringens*. Virulence 12:723-753.

Millar BC, Rao JR, Moore JE, 2021. Fighting antimicrobial resistance (AMR): Chinese herbal medicine as a source of novel antimicrobials–an update. Letters in Applied Microbiology 73:400-407.

Pielou EC, 1966. The measurement of diversity in different types of biological collections. Journal of Theoretic Biology 13:131-144.

Qi X, Lu X, Han Y, *et al*., 2023. Ginseng polysaccharide reduces autoimmune hepatitis inflammatory response by inhibiting PI3K/AKT and TLRs/NF-κB signaling pathways. Phytomedicine 116:154859.

Qiu P, Ishimoto T, Fu L, *et al*., 2022. The gut microbiota in inflammatory bowel disease. Frontiers in Cellular and Infectious Microbiology 12:733992.

Ray PD, Huang BW, Tsuji Y, 2012. Reactive oxygen species (ROS) homeostasis and redox regulation in cellular signaling. Cell Signal 24:981-990.

Rietschel ET, Westphal O, 2020. Endotoxin: historical perspectives. In: Brade H, Opal SM, Vogel SN, *et al.* (Eds.), Endotoxin in Health and Disease. 2nd Ed. CRC Press, Boca Raton, pp:1-30.

Rogers AW, Tsolis RM, Bäumler AJ, 2021. Salmonella versus the microbiome. Microbiology and Molecular Biology Reviews 85:e00027-20.

Ross J, Schatz C, Beaugrand K, *et al*., 2021. Evaluation of activated charcoal as an alternative to antimicrobials for the treatment of neonatal calf diarrhea. Veterinary Medicine Research Reports 12:359-369.

Sasidharan Pillai S, Gagnon CA, Foster C, *et al*., 2024. Exploring the gut microbiota: key insights into its role in obesity, metabolic syndrome and type 2 diabetes. Journal of Clinical Endocrinology and Metabolism 109:2709-2719.

Shannon CE, 1948. A mathematical theory of communication. Bell System Technical Journal 27:623-656.

Siddique A, Wang Z, Zhou H, *et al*., 2024. The evolution of vaccines development across Salmonella serovars among animal hosts: a systematic review. Vaccines 12:1067.

Simpson EH, 1949. Measurement of Diversity. Nature 163:688.

Su T, Qiu Y, Hua X, *et al*., 2020. Novel opportunity to reverse antibiotic resistance: to explore traditional Chinese medicine with potential activity against antibiotics-resistance bacteria. Frontiers in Microbiology 11:610070.

Troha K, Ayres JS, 2022. Cooperative defenses during enteropathogenic infection. Current Opinions in Microbiology 65:123-130.

Virzì GM, Mattiotti M, de Cal M, *et al*., 2022. Endotoxin in sepsis: methods for LPS detection and the use of omics techniques. Diagnostics 13:79.

Wang L, Zhang P, Li C, *et al*., 2022. A polysaccharide from *Rosa roxburghii* Tratt fruit attenuates high-fat diet-induced intestinal barrier dysfunction and inflammation in mice by modulating the gut microbiota. Food and Functions 13:530-547.

Wang Y, Lai W, Zheng X, *et al*., 2024. *Linderae radix* extract attenuates ulcerative colitis by inhibiting the JAK/STAT signaling pathway. Phytomedicine 132:155868.

Wen Z, Liu W, Li X, *et al*., 2019. A protective role of the NRF2-Keap1 pathway in maintaining intestinal barrier function. Oxidative Medicine and Cellular Longevity 2019:1759149.

Xie H, Yu S, Tang M, *et al*., 2025. Gut microbiota dysbiosis in inflammatory bowel disease: interaction with intestinal barriers and microbiota-targeted treatment options. Frontiers in Cellular and Infectious Microbiology 15:1608025.

Yang J, Xiong K, Li T, *et al*., 2025. Anti-inflammatory effects of natural polysaccharides: molecular mechanisms and nanotherapeutic applications. Frontiers in Immunology 16:1723346.

Yue Y, He Z, Zhou Y, *et al*., 2020. Lactobacillus plantarum relieves diarrhea caused by enterotoxin-producing *Escherichia coli* through inflammation modulation and gut microbiota regulation. Food and Functions 11:10362-10374.

Zarneshan SN, Fakhri S, Farzaei MH, *et al*., 2020. Astaxanthin targets PI3K/Akt signaling pathway toward potential therapeutic applications. Food and Chemical Toxicology 145:111714.

Zhang J, Zhao L, He J, *et al*., 2025. Protective effects of Perilla seed extract and its active ingredient luteolin against inflammatory bowel disease via the PI3K/AKT signaling pathway in-vivo and in-vitro. International Journal of Molecular Science 26:3564.

Zhang L, Gui S, Wang J, *et al*., 2020. Oral administration of green tea polyphenols (TP) improves ileal injury and intestinal flora disorder in mice with Salmonella typhimurium infection via resisting inflammation, enhancing antioxidant action and preserving tight junction. Journal of Functional Foods 64:103654.

Zhao C, Zhang Z, Nie D, *et al*., 2022. Protective effect of lemon essential oil and its major active component, D-limonene, on intestinal injury and inflammation in S. spp-challenged mice. Frontiers in Nutrition 9:843096.